CrystEngComm

PAPER

View Article Online
View Journal | View Issue

Cite this: *CrystEngComm*, 2018, **20**, 3049

Why lamivudine assembles into double-stranded helices in crystals: salt heterosynthon *versus* base-pairing homosynthon†

Cameron Capeletti da Silva, *[a] Ana K. Valdo,[a] José Antônio do Nascimento Neto,[a] Leandro Ribeiro,[a] Ariel M. Sarotti [b] and Felipe Terra Martins[a]

Received 22nd January 2018,
Accepted 20th April 2018

DOI: 10.1039/c8ce00100f

rsc.li/crystengcomm

Here we were interested in obtaining a better understanding of the competition between the salt heterosynthon and the base-pairing homosynthon formed by the anti-HIV drug lamivudine in the presence of strong acids. Even though the preparation of the multicomponent crystal forms of this drug with weak or moderate acids is well investigated, the crystallization of lamivudine with strong acids is still little explored. Besides filling this crystallization screening gap, the driving forces of the so-called lamivudine duplexes could be drawn from the complete structural landscape and the theoretical thermodynamic parameters of the salt heterosynthon, calculated at the M06-2X/6-31+G** level of theory. Five new crystal structures of lamivudine were obtained, wherein two of them were assembled as base-paired helically-stacked strands in the presence of trifluoroacetic and trichloroacetic acids (lamivudine duplexes V and VI, respectively). Besides, three salts were prepared by crystallization of lamivudine with sulfuric and perchloric acids. Finally, the theoretical approach showed that there is no energy trend regarding the formation of lamivudine duplexes with aliphatic organic acids or lamivudine salts with aromatic acids, which is usually observed in practice.

Introduction

The design of new solid forms of pharmaceutical ingredients has been well explored through crystal engineering approaches in the last few years.[1,2] In this context, the understanding of how species interact with each other in a multicomponent crystal form is a major task. In this way, crystal engineering involves the analysis of supramolecular interactions, especially hydrogen bonding patterns between entities that constitute a multicomponent system.[3–6]

Since lamivudine (β-L-2′,3′-dideoxy-3′-thiacytidine, 3TC) has been released onto the market, it has been widely studied due to its pharmacological significance. Lamivudine is a nucleobase analogue inhibitor of the reverse transcriptase enzyme and is greatly used to treat HIV and hepatitis B virus.[7] Additionally, this drug has exhibited great potential in forming multicomponent systems due to its ability to crystallize with different species, probably because of its multiple hydrogen bond donor and acceptor groups. Concerning the crystal engineering of lamivudine, many solid phases of this drug are known, including salts with inorganic and carboxylic acids (aromatic and aliphatic chains), co-crystals, salt co-crystals and polymorphs.[8]

The structural diversity of lamivudine solid phases is even demonstrated by double-helix supramolecular aggregates. Until now, there have been four crystalline structures of lamivudine duplexes reported in the literature, named as duplexes I, II, III and IV.[9] Duplex I[9a] was prepared based on a three-point synthon responsible for the assembly of lamivudine 3,5-dinitrosalicylate monohydrate salt.[8h] This hydrogen bonding pattern is responsible for the pairing between one neutral and one protonated lamivudine unit (3TC–3TC$^+$; Fig. 1b). Besides, maleic acid was used as a counterpart to crystallize with lamivudine in this solid form. Duplex II, on the other hand, was obtained by the self-assembly of neutral lamivudine pairs (3TC–3TC) in a helical fashion through only two hydrogen bonds.[9b] Duplex III was obtained by crystallizing lamivudine and fumaric acid together. The hydrogen bonding pattern responsible for keeping together the lamivudine units in this DNA-like structure is a mixture of hemiprotonated (3TC–3TC$^+$) and neutral (3TC–3TC) motifs.[9c] Another supramolecular aggregate possessing nucleobase-pairing and helical stacking as DNA-mimicry has

[a] *Instituto de Química, Universidade Federal de Goiás, Campus Samambaia, Goiânia, GO, CP 131, 74001-970, Brazil. E-mail: cameron.capeletti@gmail.com*
[b] *Instituto de Química Rosario (IQUIR), Universidad Nacional de Rosario–CONICET, Suipacha 531, S2002LRK Rosario, Argentina*

† Electronic supplementary information (ESI) available: PDF file including Fig. S1–S4 and Tables S1–S12. CCDC crystal data in CIF file format (CCDC 1580051–1580055). For ESI and crystallographic data in CIF or other electronic format see DOI: 10.1039/c8ce00100f

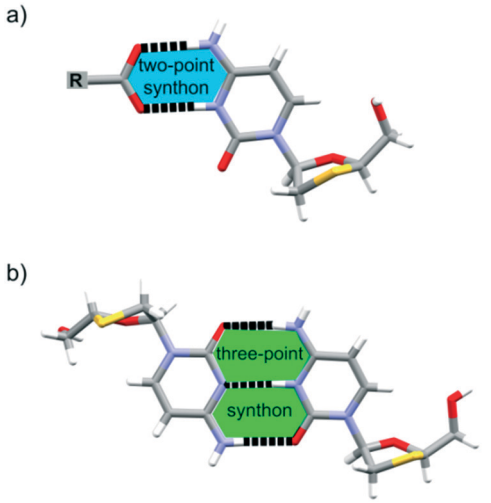

Fig. 1 Hydrogen bonding pattern in lamivudine structures with organic acids: (a) lamivudine (3TC$^+$) and (b) hemiprotonated motifs (3TC–3TC$^+$). Letter R denotes any group on the organic acid.

been reported in duplex IV, which is made up of 3TC–3TC$^+$ pairs and D-tartrate as counterions.[9d]

Based on the fact that lamivudine can promptly crystallize with acids through either the two-point heterosynthon (common in lamivudine salts) or the three-point homosynthon (common in lamivudine duplexes), we were interested in obtaining a better understanding of the competition between these hydrogen bonding patterns (Fig. 1). In this context, it was necessary to fill a gap in the solid state chemistry of the drug, seeing that there was scarce observance of crystallization of lamivudine with strong acids. The crystallization of lamivudine with strong acids is still little explored; however, the preparation of the multicomponent systems of this drug with weak or moderate acids is well investigated.[8,9] Once this gap is filled, we would have a complete range of structures, from which we could extract the structural knowledge that leads to the formation of the three-point homosynthon or two-point heterosynthon. In this way, we selected a set of strong acids, trifluoroacetic acid, trichloroacetic acid, sulfuric acid and perchloric acid to be exact, to crystallize with lamivudine (Scheme 1). Five new crystal structures of lamivudine are reported here, *i.e.*, two lamivudine duplexes prepared with trifluoroacetic and trichloroacetic acids, respectively, and three molecular salts formed by lamivudine crystallization with sulfuric and perchloric acids. Lamivudine duplexes with trifluoroacetic and trichloroacetic acids were named duplexes V and VI, respectively. Three lamivudine salts were obtained with sulfuric acid (lamivudine sulfate and lamivudine hydrogen sulfate) and perchloric acid (lamivudine perchlorate monohydrate). Finally, aided by theoretical calculations of key thermodynamic parameters for the heterosynthon present in salts, at the M06-2X/6-31+G** level of theory, this study allowed us to investigate the tendency of lamivudine to crystallize into a double-helical arrangement.

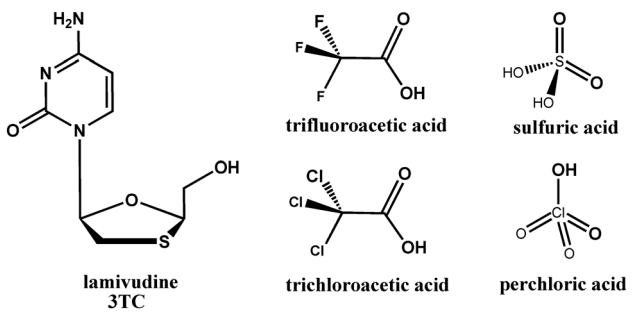

Scheme 1 Lamivudine and the strong acids used in this study.

Experimental section

Materials and methods

Preparation. The preparation of all solid phases reported here was carried out using lamivudine form II as follows. Lamivudine duplex V: 20.00 mg (0.087 mmol) of lamivudine was dissolved in 5 mL of methanol, followed by addition of 100 μL of aqueous solution of trifluoroacetic acid (0.4 mol L^{-1}, 0.04 mmol) while stirring. The solution was allowed to evaporate slowly at room temperature, yielding crystals in 4 days. Lamivudine duplex VI, sulfate, and perchlorate monohydrate salts of lamivudine were prepared similarly to duplex V, although solutions (100 μL) of trichloroacetic acid, sulfuric acid and perchloric acid were used instead, at the same concentration of the trifluoroacetic acid solution mentioned before. The preparation of lamivudine hydrogen sulfate also resembles that just described here, although 200 μL of an aqueous solution of sulfuric acid (0.4 mol L^{-1}, 0.08 mmol) was added to the solution of lamivudine. After 4 days, crystals of the new multicomponent systems were obtained in a glass vial.

Structure determination. All data were collected using a Bruker-AXS Kappa Duo diffractometer equipped with an APEX II CCD detector after exposure to MoKα radiation (0.71073 Å). Then, the raw data sets were treated using SAINT and SADABS[10] programs for cell refinement and data reduction. Next, the structures were solved by direct methods of phase retrieval with SHELXS-2014[11] and then refined with SHELXL-2014 (ref. 11) using the full-matrix least-squares method on F^2. All non-hydrogen atoms were refined with free anisotropic displacement parameters while the hydrogen atoms had their displacement parameters fixed and set to isotropic. The hydrogen atoms were positioned according to both intramolecular and intermolecular requirements and constrained following a riding model. In the structures of duplexes V and VI, the molecules of lamivudine and counterions were very disordered. Consequently, the necessary restraints and constraints were used in their refinement. Their single crystals have diffracted X-rays poorly even at the medium resolution shell. Besides, in the structure of lamivudine hydrogen sulfate, residual electron density was observed in the void present in its crystal lattice. Then, PLATON/SQUEEZE was also used to treat this diffraction dataset. Also, the disordered oxygen atoms of hydrogen sulfate and perchlorate anions were modeled over two sets of 50% occupancy. For clarity reasons, in the crystal

structure representations, only the atoms of one set were depicted. Finally, for structure analysis and graphical representations the following programs were used: MERCURY[12] and CHIMERA.[13] The thermal ellipsoid plot of the crystal structures reported here and the details of the single crystal X-ray diffraction experiment are in the ESI† (Fig. S1 and S2 and Table S1). Tables S2–S6† display the main hydrogen bonding geometry found in the structures of duplex V, duplex VI, lamivudine sulfate, lamivudine hydrogen sulfate and lamivudine perchlorate monohydrate, respectively.

Theoretical calculations. Since all known lamivudine duplexes are assembled with aliphatic organic acids, while aromatic organic acids assemble the $R_2^2(8)$ heterosynthon, a hypothesis was raised, concerning the energetic difference for this synthon in these two classes of acids. For this reason, we were interested in probing their thermodynamic properties through theoretical calculations at the M06-2X/6-31+G** level of theory.[14] Some lamivudine aggregates were extracted from the crystal structures found in the CSD database, while others were created using Chimera[13] since they were not available in the crystal structures of lamivudine. The energy was calculated without optimization, after partial optimization (only hydrogen atoms) and after full geometric optimization of heterodimers formed by the in-plane pairing of lamivudine (3TC) or lamivudinium ($3TC^+$) and organic acids as counterions. The thermodynamic properties such as Gibbs energy, enthalpy and entropy were also calculated after full optimization of lamivudine heterodimers.

Thermal analysis (TG and DTA). Samples of lamivudine duplex V and duplex VI have been characterized by simultaneous application of thermogravimetry (TG) and differential thermal analysis (DTA). The thermal analysis was carried out on a Shimadzu® DTG-60 thermal analyzer, where the samples were loaded into alumina crucibles. The samples were heated from 25 °C to 450 °C with a heating rate of 10° min^{-1} under a dynamic air atmosphere at a flow rate of 50 mL min^{-1}. The results are presented in Fig. S3 and S4 in the ESI.†

Results and discussion

Lamivudine duplex V

Lamivudine duplex V was prepared by drug crystallization with trifluoroacetic acid. This structure was solved in the $P3_2$ space group of the trigonal crystal system with eight hemiprotonated base pairs (3TC–$3TC^+$) in the asymmetric unit. The asymmetric unit of the antecedent duplex I comprised four base pairs, while duplex III was composed of a mixture of hemiprotonated and neutral base-pairing motifs present in a 4 : 1 ratio. On the other hand, duplex IV exhibited only one base pair in its asymmetric unit.[9] Besides, other species crystallized together with the drug molecules in the crystal lattice of duplex V. Eight trifluoroacetate anions and four water molecules are present in the crystal structure of the trigonal duplex V.

Another feature present in the nucleoside double-stranded helix reported here, which is similar to the preceding duplexes I, III and IV, concerns the hydrogen bonding pattern responsible for the in-plane pairing of the drug units. The three-point synthon is responsible for holding the lamivudine base pairs together (3TC–$3TC^+$) (Fig. 1b). This synthon is constructed by two N–H···O hydrogen bonds in the periphery and one N^+–H···N hydrogen bond in the center. In addition to displaying the nucleobase pairing, this crystal structure also shows the helical stacking of the hemiprotonated (3TC–$3TC^+$) units of lamivudine giving rise to a DNA-like double helix structure. The lamivudine pairs present in duplex V are stacked on top of each other in a face-to-face fashion (Fig. 2). Such a stacking pattern also occurs in duplexes I, III and IV.

Aside from these similarities among lamivudine duplexes, it is interesting to observe that duplex V is the first DNA-like nucleoside structure with two crystallographically independent double-stranded helices within the crystal lattice (Fig. 2). The labeling scheme of the drug units was made using the capital letters A, B, C and so on, until P. The first duplex motif is made up of lamivudine units labeled from A to L (motif AL), while the second one comprises lamivudine molecules M to P (motif MP). Concerning the content per helical turn, both duplex motifs are very similar, since they are made up of six 3TC–$3TC^+$ pairs spaced by *ca.* 3.4 Å each. Also, both duplex motifs are left-handed, as in the structures of lamivudine duplexes I and III.[9a,c] However, it is worth noting that in the MP motif, four lamivudine pairs are generated by 3_2-screw axis symmetry. An entire turn measures about 20.4 Å for both duplex motifs AL and MP, respectively. Therefore, a complete helical turn in duplex V motifs is smaller than those observed in duplexes I and III (25.60 Å and 33.69 Å, respectively).[9a,c]

The trifluoroacetate anions and water molecules help stabilize the duplex V motifs by interacting with the cytosine ring and the 5′-CH_2OH groups of lamivudine units through classical hydrogen bonds. The hydrogen bonding geometry in duplex V is shown in Table S2.† The disposition of the counterions and water molecules surrounding the grooves gives rise to layers and channels in the crystal structure of duplex V (Fig. 2). The occurrence of these channels also resembles the reported structures of duplexes III and IV.[9c,d]

Lamivudine duplex VI

Continuing our crystallization assays of lamivudine with strong acids, we have prepared another double-stranded helix of lamivudine (lamivudine duplex VI). This duplex was obtained using trichloroacetic acid and crystallized in the hexagonal space group $P6_1$ with two hemiprotonated 3TC–$3TC^+$ base pairs, two trichloroacetate anions and one water molecule in the asymmetric unit. The nomenclature of the species found in this structure follows that in duplex V, but in this case, lamivudine molecules were labeled from A to D, and the counterions were named XA and XB, while the water oxygen was labeled O1w.

Lamivudine duplex VI displays some characteristics that resemble those already reported in the literature[9] and also those

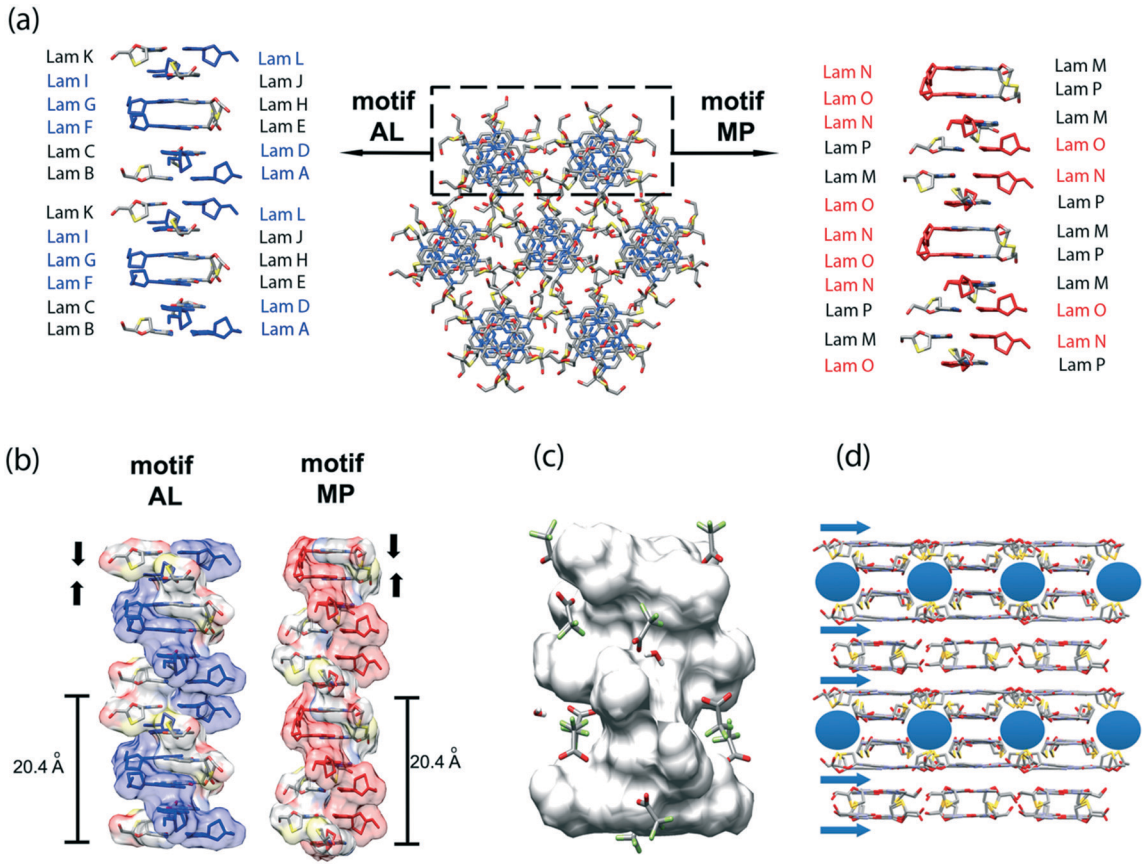

Fig. 2 (a) Top view of lamivudine duplex V outlining the two crystallographically independent duplex motifs AL and MP. Lamivudine molecules of two unit cells are shown. (b) Surface rendering of duplex V motifs is also exhibited. The black arrows indicate the face-to-face stacking of the drug units. Hydrogen atoms, trifluoroacetate anions and water molecules were hidden for clarity reasons. (c) The trifluoroacetate anions and water molecules surrounding a complete helical turn in duplex V (motif MP). (d) The layers and channels filled with trifluoroacetate anions and water molecules are highlighted.

of duplex V, due to the occurrence of the same hydrogen bonding and stacking patterns. This duplex is assembled by the three-point homosynthon (Fig. 1), in which one protonated lamivudine is paired with a neutral one. Besides, all lamivudine dimers are stacked on top of one another in a face-to-face manner. Lamivudine duplex VI shows only one independent duplex motif (Fig. 3), which is also left-handed, as observed in some previously reported duplex structures.[9a,c] Despite these similarities, the structure of lamivudine duplex VI has some differences when compared with the other lamivudine duplexes. For example, this DNA-like duplex has the largest number of lamivudine dimers per helical turn known so far. Duplex VI has twelve lamivudine base pairs in a complete helical turn, measuring about 42.00 Å. Eight, nine and ten lamivudine base pairs were found in a complete helical turn for duplexes I, II and III, respectively.[9a–c] An entire turn of lamivudine duplex V was composed of six dimers of the drug.

As exhibited in lamivudine duplex V, the counterions and water molecules also play an important role in the stabilization of the double-stranded helix VI (Fig. 3). Two neighboring duplexes are interlinked through the interactions between the drug units and the counterions touching the grooves. In a similar way to that occurring in duplex V, channels filled with counterions and water molecules are found in duplex VI, wherein each motif alternates with the channels (Fig. 3).

It is important to mention that thermogravimetry (TG) and differential thermal analysis (DTA) were performed for the structures of duplexes V and VI. The thermograms show that duplexes V and VI start losing water at 103.0 °C and 64.9 °C (DTA onset temperatures), respectively. The mass losses of duplexes V (1.5%) and VI (1.2%) associated with the elimination of water molecules are consistent with the calculated ones from the crystal structures (1.5% and 1.4% for duplexes V and VI, respectively). After losing water, lamivudine duplex VI also exhibits the loss of the trichloroacetic acid species at 99.8 °C. The found mass loss attributed to them (24.6%) also agrees with the calculated one (25.7%). Thus, based on these thermal analyses, duplex V is more stable than duplex VI upon heating. Their thermograms can be seen in Fig. S3 and S4 in the ESI.†

Lamivudine sulfate

In the course of our attempt to expand the landscape of lamivudine structures with strong acids, we have obtained a

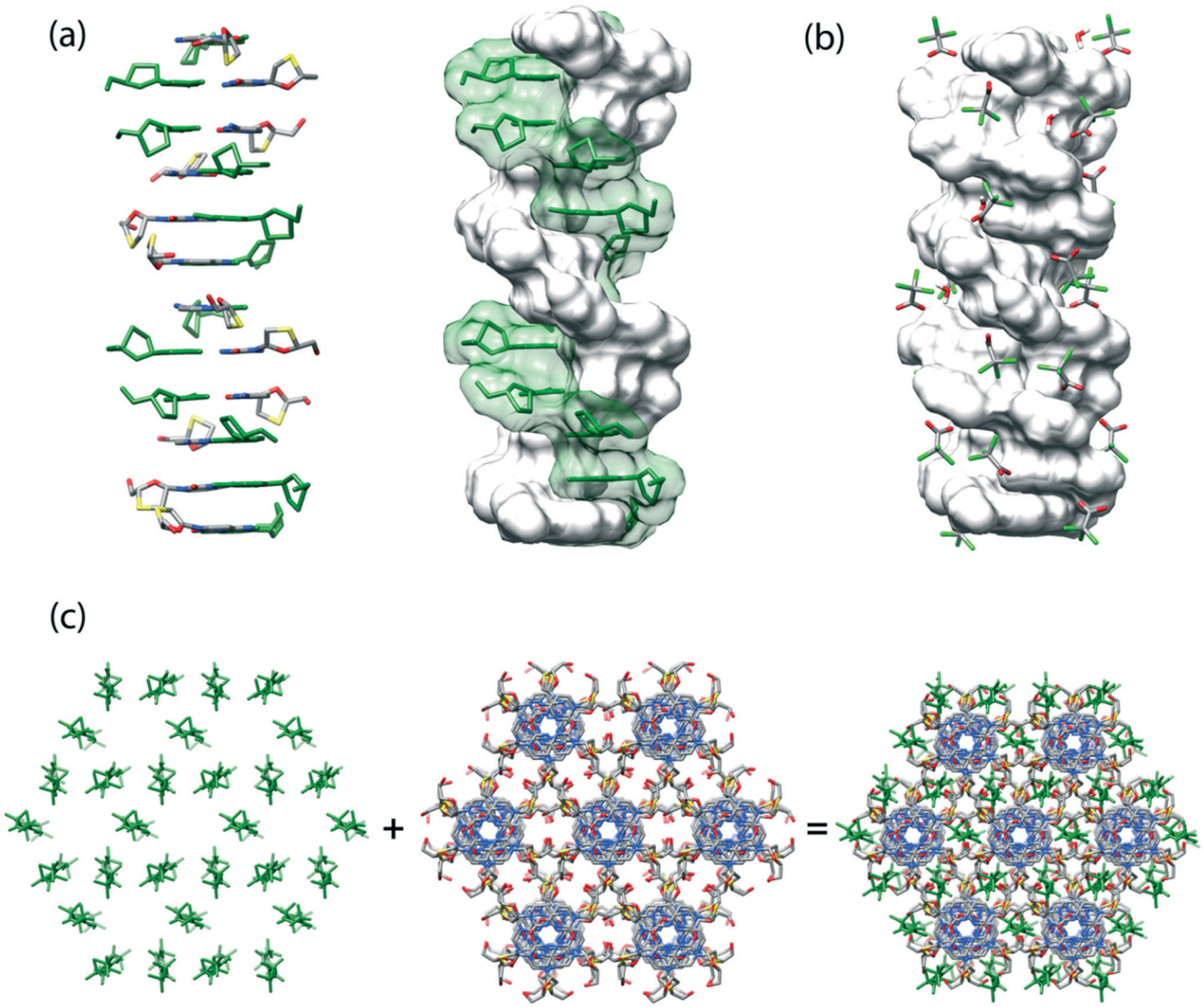

Fig. 3 (a) A complete helical turn of lamivudine duplex VI outlining the two strands of this double helix structure. The surface rendering of duplex VI is also displayed. The hydrogen atoms, trichloroacetate anions and water molecules were hidden for clarity reasons. (b) Trichloroacetate anions and water molecules interacting with NH_2 hydrogen atoms not involved in the base pairing and 5′-OH groups of lamivudine units. (c) Top view of the duplex VI structure with anions and water molecules alternating with the duplex motifs.

new salt form of this drug under acidic conditions. It is a sulfate salt, whose crystal structure was solved in the orthorhombic space group $P2_12_12_1$. The asymmetric unit of lamivudine sulfate is composed of two lamivudinium cations along with a fully deprotonated sulfate anion (Fig. 4a). A two-point synthon described by the graph set notation $R_2^2(8)$ is seen on both sides of the sulfate anion. This synthon is similar to the ring motif shown in Fig. 1a. The $R_2^2(8)$ heterosynthon was assembled due to the protonated cytosine ring of lamivudine being involved in intermolecular interactions through its amine and imine functionalities with two oxygen atoms of the sulfate anion (Fig. 4a). Additional interactions between the cation and the anion are also observed, which, along with those described in the $R_2^2(8)$ salt heterosynthon, are responsible for assembling sheets intercalating lamivudinium and sulfate species (Fig. 4b). Besides, these sheets are held together by interactions between the 5′-OH groups of neighboring lamivudine units and also between the 5′-OH group and the sulfate anion.

Lamivudine hydrogen sulfate

Lamivudine hydrogen sulfate also crystallized in the space group $P2_12_12_1$, as the lamivudine sulfate. The asymmetric unit of this structure exhibits one lamivudinium entity and a hydrogen sulfate anion. The protonation pattern of the counterion found in this crystal form differs from that of the parent salt with sulfate. In this case, the sulfate anion is present in the monoprotonated form instead of a divalent anion (Fig. 5). The $R_2^2(8)$ heterosynthon is once more the main synthon, however, this time, it is present only at one side of the hydrogen sulfate anion. An adjacent lamivudine molecule

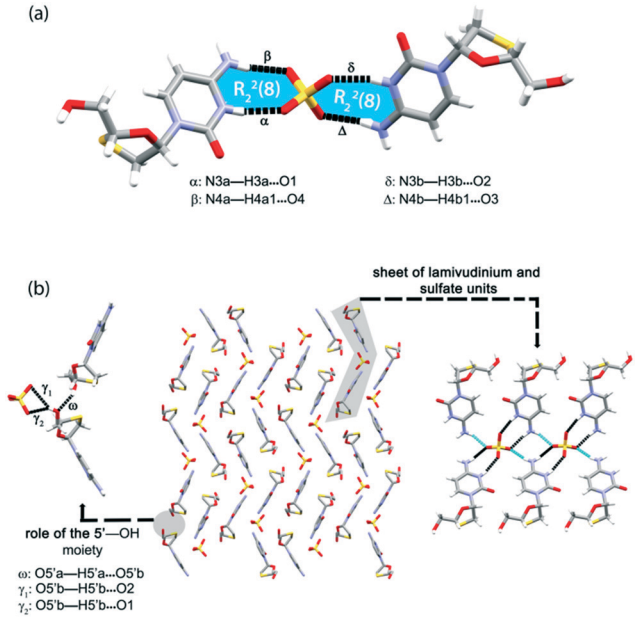

Fig. 4 (a) Asymmetric unit of lamivudine sulfate highlighting the $R_2^2(8)$ heterosynthon, which is responsible for the pairing between the drug and the counterion. (b) Zigzag packing motif of the lamivudine sulfate structure showing sheets of lamivudinium and sulfate species and also the role of the 5′-OH groups. The hydrogen bonds assembling the two-point synthon are colored in black, while the interaction of the hydrogen not involved in the pairing is shown in cyan.

is engaged on the other side as a bifurcated hydrogen bond donor, through its NH_2 hydrogen, which is not involved in the $R_2^2(8)$ synthon, to hydrogen sulfate oxygen atoms (Fig. 5).

The 5′-OH group of lamivudine is also involved in hydrogen bonding donation to one hydrogen sulfate oxygen engaged in the $R_2^2(8)$ synthon. The hydrogen bonding network resulting from this overall hydrogen bonding pattern gives rise to sheets resembling those present in the structure of the sulfate salt. The stacking of these sheets generates a layered structure onto the *bc* plane, where structural voids are also located (Fig. 5).

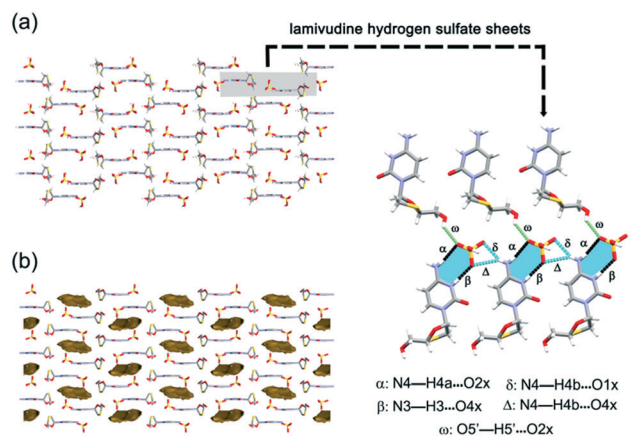

Fig. 5 (a) Packing of the layered structure of lamivudine hydrogen sulfate. A sheet made up of lamivudinium and hydrogen sulfate species is highlighted, wherein the $R_2^2(8)$ heterosynthon is displayed as black contacts, the bifurcated hydrogen bonds are shown in cyan, and the hydrogen bond involving the 5′-OH group is shown in light green. (b) Another crystal packing view of the hydrogen sulfate salt showing the voids between the layers made up of lamivudine and hydrogen sulfate units.

Lamivudine perchlorate monohydrate

Lamivudine perchlorate monohydrate crystallized in the space group $P2_12_12_1$ as the sulfate and hydrogen sulfate salts. It would be expected that this salt forms the $R_2^2(8)$ synthon as observed for lamivudine structures with sulfate and hydrogen sulfate anions. However, the crystal packing of lamivudine perchlorate monohydrate differs profoundly from the salt structures just described in this work. Neither the two-point synthon nor the three-point one is seen in this crystal structure. This lamivudine salt has infinite chains made up of protonated lamivudine, water and perchlorate species (Fig. 6b). The structure of lamivudine perchlorate monohydrate shows an $R_2^1(6)$ homosynthon, in which the imine and amine groups are hydrogen bond donors to the carbonyl moiety of a neighboring lamivudinium cation from an adjacent chain (Fig. 6a). Chains are assembled through bifurcated hydrogen bonds between the drug and counterion and also by two interactions whose water acts as the hydrogen bonding donor to both lamivudinium and perchlorate (Fig. 6b). Neighboring

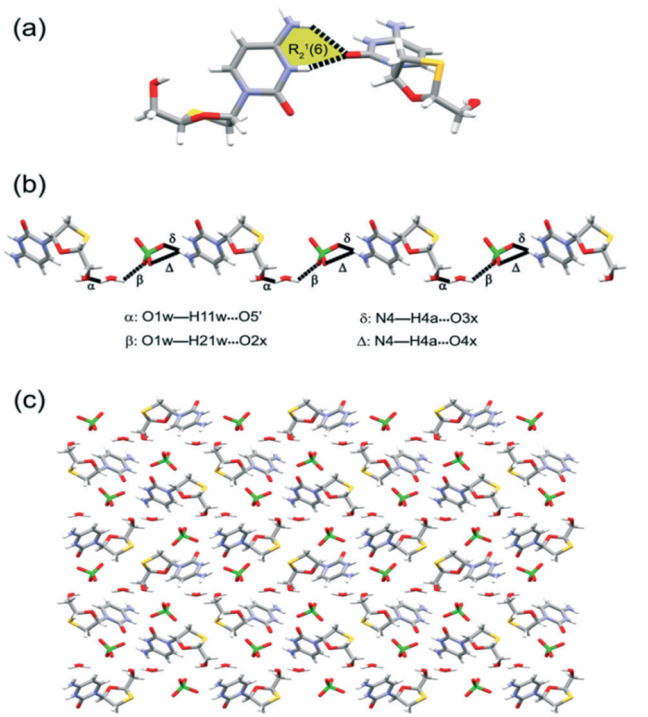

Fig. 6 (a) Supramolecular synthon found in lamivudine perchlorate monohydrate. (b) Chain made up of lamivudinium, water and perchlorate species. The hydrogen bonding array responsible for the assembly of the chain is described. (c) Packing of the layered structure of lamivudine perchlorate monohydrate.

chains are arranged parallel to each other along the *bc* plane giving rise also to a layered structure (Fig. 6c).

CSD search and synthon analysis

In this work, five new crystalline structures of lamivudine are provided. All solid state phases were obtained using strong acids, in which two of them were assembled as DNA-like duplexes with a 3TC–3TC$^+$ motif, while the other three did not exhibit this arrangement, which were composed only of lamivudinium (3TC$^+$) species. This outcome shows that lamivudine can form multicomponent systems with either protonated (3TC$^+$) or hemiprotonated (3TC–3TC$^+$) motifs, in which either the robust $R_2^2(8)$ heterosynthon or the three-point synthon is present, respectively. It is worth mentioning that the synthesis of lamivudine duplexes was only achieved when the organic acids with aliphatic chains were used. When the inorganic species were employed instead, the resulting structures displayed different hydrogen bonding patterns, wherein the $R_2^2(8)$ heterosynthon was prevalent.

Therefore, with the purpose of evaluating the conditions that could lead to the formation of lamivudine duplexes instead of lamivudiniun salts, we firstly carried out a Cambridge Structural Database[15] (CSD, version 5.38 updated in May 2017) survey of the lamivudine solid state phases. This search was performed in order to analyze the previous structures of lamivudine that crystallized out from acid medium and to assess the most frequent synthons present in such multicomponent systems. A total of 33 hits for structures containing lamivudine fragment was found, but only those with organic acids (16 entries) were considered for synthon analysis (Table 1). Seven structures have been observed for lamivudine crystal forms with aromatic carboxylic acids, while nine entries are present with aliphatic organic acids. In this CSD analysis, six structures containing aromatic acids exhibit the $R_2^2(8)$ synthon. Since a conjugated unsaturated system is present in all these structures of lamivudine with aromatic acids, the formation of this robust synthon could have been favored due to the presence of resonance-assisted hydrogen bonding (RAHB).[16]

If all hits for organic acids are considered, then 11 hits (69%) have the two-point heterosynthon, which can be correlated with previous reports demonstrating the high occurrence of the $R_2^2(8)$ heterosynthon in multicomponent crystal systems of cytosine.[17–19] The robustness of this synthon is also observed in the structures reported here for lamivudine salts with sulfuric acid, wherein two hydrogen bonds (N···H–O) are responsible for the in-plane pairing between lamivudinium and the sulfate anion.

In contrast, lamivudine duplex formation could have been supported due to the lack of RAHB in aliphatic acids employed in their preparation. Thus, the two duplexes with trifluoroacetic and trichloroacetic acids reported here are in agreement with this assumption.

Another valuable observation concerns two already published structures of lamivudine with maleic acid (CSD refcodes BUYFAD[9a] and CUNVUD01 (ref. 8*b*)). Lamivudine self-assembles a DNA-like duplex in the presence of maleic acid.[9a] On the other hand, the $R_2^2(8)$ heterosynthon can be also formed between lamivudine and maleic acid in another structure.[8b] This dual behavior can be explained by the geometrical features of maleic acid. Maleic acid is a moderate organic acid possessing a C=C double bond in *cis* configuration. This keeps the carboxyl groups close together, being able to perform RAHB. For this reason, it can be placed between aromatic and aliphatic acids as a middle ground, and consequently it can favor both lamivudine duplex and salt formation. Meanwhile, only one lamivudine duplex is formed with a *trans* isomer present without RAHB, namely, fumaric acid (CSD refcode WONGUD[9c]).

Therefore, since lamivudine duplexes are assembled with aliphatic organic acids, while aromatic ones assemble the $R_2^2(8)$ heterosynthon with the drug, the energy of this heterosynthon in these two classes of acids was expected to be

Table 1 Hydrogen bonding pattern of lamivudine in multicomponent systems with organic acids

Refcode	Aromatic acids	Synthon	References	Refcode	Aliphatic acids	Synthon	References
COWSUD	3,5-Dinitrosalicylic acid	Three-point	Bhatt *et al.*, 2005 (ref. 8*h*)	BUYFAD	Maleic acid (duplex I)	Three-point	Martins *et al.*, 2010 (ref. 9*a*)
GAXFOC	Phthalic acid	$R_2^2(8)$	Silva *et al.*, 2012 (ref. 8*c*)	WONGUD	Fumaric acid (duplex III)	Three-point	Vasconcelos *et al.*, 2014 (ref. 9*c*)
GAXFUI	Salicylic acid	$R_2^2(8)$	Silva *et al.*, 2012 (ref. 8*c*)	UYEZAB	D-Tartaric acid (duplex IV)	Three-point	Silva and Martins 2016 (ref. 9*d*)
HOSMAF	R-Mandelic acid	$R_2^2(8)$	Silva and Martins 2015 (ref. 8*k*)	UYEYEE	L-Tartaric acid	$R_3^2(8)$	Silva and Martins 2016 (ref. 9*d*)
RIBFIT	Phthalic acid	$R_2^2(8)$	Silva *et al.*, 2013 (ref. 8*d*)	VISWAX	Pimelic acid	$R_2^2(8)$	Chakraborty *et al.*, 2014 (ref. 8*i*)
RIBFOZ	4,5-Dichlorophthalic acid	$R_2^2(8)$	Silva *et al.*, 2013 (ref. 8*d*)	CUNVUD01	Maleic acid	$R_2^2(8)$	Martins *et al.*, 2009 (ref. 8*b*)
YUBTEW	Mandelic acid	$R_2^2(8)$	Silva and Martins 2015 (ref. 8*k*)	ROQPEU	Oxalic acid	$R_2^2(8)$	Perumalla and Sun 2014 (ref. 8*j*)
				VISVOK	Oxalic acid	$R_2^2(8)$	Chakraborty *et al.*, 2014 (ref. 8*i*)
				VISVUQ	Oxalic acid	$R_2^2(8)$	Chakraborty *et al.*, 2014 (ref. 8*i*)

different. In order to assess if there was a thermodynamic preference for the $R_2^2(8)$ heterosynthon in lamivudine systems with aromatic organic acids, the energy of this synthon was calculated in lamivudine heterodimers with all organic acids present in duplexes and salts of the drug. The pairs formed by lamivudine and aromatic acids would be expected to be more stable than those formed with aliphatic acids, wherein the maleic acid pair would be placed in the middle of the energetic ranking. Tables S7–S9 in the ESI† show respectively the energy of the heterosynthon calculated without optimization, with partial optimization and with full geometric optimization of the aggregates extracted from the crystal structures or created using Chimera[13] when they were not available in solid forms of lamivudine. Tables S10 and S11 in the ESI† show the thermodynamic properties (Gibbs free energy, enthalpy and entropy) calculated for heterodimers after full geometric optimization. After careful analysis of these results, it is clear that there is no thermodynamic competition between the two-point and three-point synthons in lamivudine systems with organic acids. One could think that the $R_2^2(8)$ heterosynthon would have higher energy for counterions assembling duplex structures (in general, aliphatic chain acids), while the lower energy $R_2^2(8)$ heterosynthon would be expected for counterions not assembling duplexes (in general, aromatic acids). However this energy expectation was not realized, as well as other thermodynamic parameters such as enthalpy, Gibbs free energy and entropy. This can be observed since there is no grouping of thermodynamic parameter values according to the ability of counterions to assemble or not assemble duplex structures (Tables S7–S11†).

Therefore, our results strengthen the findings found by Perumalla *et al.*,[8j,18,19] where the formation of the three-point homosynthon by controlling the amount of the acid in the crystallization was demonstrated. As a result, the formation of lamivudine supramolecular aggregates possessing nucleobase-pairing and helical stacking seems to be related to the organic acid availability.[18,19] Finally, the formation of lamivudine duplexes does not depend on the strength of the acids (pK_a (ref. 20)), as can be seen in Table S12 in the ESI.† ΔpK_a values for each multicomponent system also show that there is no direct relationship between the duplex formation and the acidity difference between lamivudine and its coformers (Table S12†).

Conclusions

In this study, five multicomponent crystal forms of lamivudine with strong acids were characterized by the single crystal X-ray diffraction technique. Lamivudine duplexes V and VI were assembled as base-paired helically-stacked strands, while sulfate, hydrogen sulphate and perchlorate monohydrate salts did not present either base-pairing or helical base-stacking. Another interesting feature lies in the formation of the duplex structure regardless of the acid strength because there is formation of such structures with strong, moderate and weak acids, as well as with no acids at all. Besides, our theoretical approach showed that there is no thermodynamic trend regarding the commonly found formation of lamivudine duplexes with aliphatic organic acids or lamivudine salts with aromatic ones.

Conflicts of interest

There are no conflicts to declare.

Acknowledgements

The authors thank the Brazilian Research Council CNPq (Conselho Nacional de Desenvolvimento Científico e Tecnológico) and FAPEG (Fundação de Amparo à Pesquisa do Estado de Goiás) for financial support (Processo CNPq 445802/2014-6 and Processo FAPEG 15291). C. C. S. also thanks FAPEG for the doctoral scholarship (Processo 201410267000635). F. T. M. also thanks CNPq for the research fellowship.

Notes and references

1 N. K. Duggirala, M. L. Perry, O. Almarsson and M. J. Zaworotko, *Chem. Commun.*, 2016, **52**, 640–655.
2 S. Cherukuvada, R. Kaur and T. N. Guru Row, *CrystEngComm*, 2016, **18**, 8528–8555.
3 E. J. C. de Vries, S. Kantengwa, A. Ayamine and N. B. Báthori, *CrystEngComm*, 2016, **18**, 7573–7579.
4 B. Sarma and B. Saikia, *CrystEngComm*, 2014, **16**, 4753–4765.
5 G. R. Desiraju, *Angew. Chem., Int. Ed. Engl.*, 1995, **34**, 2311–2327.
6 M. C. Etter, *Acc. Chem. Res.*, 1990, **23**, 120–126.
7 (*a*) L. Menendez-Arias and M. Alvarez, *Antiviral Res.*, 2014, **102**, 70–86; (*b*) J. A. V. Coates, N. Cammack, H. J. Jenkinson, I. M. Mutton, B. A. Pearson, R. Storer, J. M. Cameron and C. R. Penn, *Antimicrob. Agents Chemother.*, 1992, **36**, 202–205.
8 (*a*) R. Banerjee, P. M. Bhatt, N. V. Ravindra and G. R. Desiraju, *Cryst. Growth Des.*, 2005, **5**, 2299–2309; (*b*) F. T. Martins, N. Paparidis, A. C. Doriguetto and J. Ellena, *Cryst. Growth Des.*, 2009, **9**, 5283–5292; (*c*) C. C. da Silva, R. R. Coelho, M. L. Cirqueira, A. C. C. de Melo, I. M. L. Rosa, J. Ellena and F. T. Martins, *CrystEngComm*, 2012, **14**, 4562–4566; (*d*) C. C. da Silva, M. L. Cirqueira and F. T. Martins, *CrystEngComm*, 2013, **15**, 6311–6317; (*e*) J. Ellena, N. Paparidis and F. T. Martins, *CrystEngComm*, 2012, **14**, 2373–2376; (*f*) F. T. Martins, R. S. Corrêa, A. A. Batista and J. Ellena, *CrystEngComm*, 2014, **16**, 7013–7022; (*g*) J. C. T. Clavijo, F. F. Guimarães, J. Ellena and F. T. Martins, *CrystEngComm*, 2015, **17**, 5187–5194; (*h*) P. M. Bhatt, Y. Azim, T. S. Thakur and G. R. Desiraju, *Cryst. Growth Des.*, 2009, **9**, 951–957; (*i*) S. Chakraborty, S. Ganguly and G. R. Desiraju, *CrystEngComm*, 2014, **16**, 4732–4742; (*j*) S. R. Perumalla and C. C. Sun, *Cryst. Growth Des.*, 2014, **14**, 3990–3995; (*k*) C. C. da Silva and F. T. Martins, *RSC Adv.*, 2015, **5**, 20486–20490; (*l*) R. K. Harris, R. R. Yeung, R. B.

Lamont, R. W. Lancaster, S. M. Lynn and S. E. Staniforth, *J. Chem. Soc., Perkin Trans. 2*, 1997, **12**, 2653–2660; (*m*) A. Bhattacharya, B. N. Roy, G. P. Singh, D. Srivastava and A. K. Mukherjee, *Acta Crystallogr., Sect. C: Cryst. Struct. Commun.*, 2010, **66**, o329–o333.

9 (*a*) F. T. Martins, A. C. Doriguetto and J. Ellena, *Cryst. Growth Des.*, 2010, **10**, 676–684; (*b*) J. Ellena, M. D. Bocelli, S. B. Honorato, A. P. Ayala, A. C. Doriguetto and F. T. Martins, *Cryst. Growth Des.*, 2012, **12**, 5138–5147; (*c*) A. T. Vasconcelos, C. C. da Silva, L. H. Q. Júnior, M. J. Santana, V. S. Ferreira and F. T. Martins, *Cryst. Growth Des.*, 2014, **14**, 4691–4702; (*d*) C. C. da Silva and F. T. Martins, *CrystEngComm*, 2016, **18**, 8115–8124; (*e*) V. Kulikov, N. A. B. Johnson, A. J. Surman, M. Hutin, S. M. Kelly, M. Hezwani, D.-L. Long, G. Meyer and L. Cronin, *Angew. Chem., Int. Ed.*, 2016, **55**, 1–6.

10 *SADABS, APEX2 and SAINT*, Bruker AXS Inc., Madison, Wisconsin, USA, 2009.

11 G. M. Sheldrick, *Acta Crystallogr., Sect. A: Found. Crystallogr.*, 2008, **64**, 112–122.

12 I. J. Bruno, J. C. Cole, P. R. Edgington, M. K. Kessler, C. F. Macrae, P. McCabe, J. Pearson and R. Taylor, *Acta Crystallogr., Sect. B: Struct. Sci.*, 2002, **58**, 389–397.

13 E. F. Pettersen, T. D. Goddard, C. C. Huang, G. S. Couch, D. M. Greenblatt, E. C. Meng and T. E. Ferrin, *J. Comput. Chem.*, 2004, **25**, 1605–1612.

14 (*a*) Y. Zhao and D. G. Truhlar, *Theor. Chem. Acc.*, 2008, **120**, 215–241; (*b*) J. A. Plumley and J. J. Dannerberg, *J. Comput. Chem.*, 2011, **32**, 1519–1527; (*c*) M. J. Frisch, G. W. Trucks, H. B. Schlegel, G. E. Scuseria, M. A. Robb, J. R. Cheeseman, G. Scalmani, V. Barone, B. Mennucci, G. A. Petersson, H. Nakatsuji, M. Caricato, X. Li, H. P. Hratchian, A. F. Izmaylov, J. Bloino, G. Zheng, J. L. Sonnenberg, M. Hada, M. Ehara, K. Toyota, R. Fukuda, J. Hasegawa, M. Ishida, T. Nakajima, Y. Honda, O. Kitao, H. Nakai, T. Vreven, J. A. Montgomery Jr., J. E. Peralta, F. Ogliaro, M. Bearpark, J. J. Heyd, E. Brothers, K. N. Kudin, V. N. Staroverov, R. Kobayashi, J. Normand, K. Raghavachari, A. Rendell, J. C. Burant, S. S. Iyengar, J. Tomasi, M. Cossi, N. Rega, J. M. Millam, M. Klene, J. E. Knox, J. B. Cross, V. Bakken, C. Adamo, J. Jaramillo, R. Gomperts, R. E. Stratmann, O. Yazyev, A. J. Austin, R. Cammi, C. Pomelli, J. W. Ochterski, R. L. Martin, K. Morokuma, V. G. Zakrzewski, G. A. Voth, P. Salvador, J. J. Dannenberg, S. Dapprich, A. D. Daniels, Ö. Farkas, J. B. Foresman, J. V. Ortiz, J. Cioslowski and D. J. Fox, *Gaussian 09*, Gaussian, Inc., Wallingford, CT, USA, 2009.

15 C. R. Groom, I. J. Bruno, M. P. Lightfoot and S. C. Ward, *Acta Crystallogr., Sect. B: Struct. Sci., Cryst. Eng. Mater.*, 2016, **72**, 171–179.

16 (*a*) J. M. Guevara-Vela, E. Romero-Montalvo, A. Costales, A. M. Pendás and T. Rocha-Rinza, *Phys. Chem. Chem. Phys.*, 2016, **18**, 26383–26390; (*b*) T. M. Krygowski and J. E. Zachara-Horeglad, *Tetrahedron*, 2009, **65**, 2010–2014; (*c*) K. T. Mahmudov and A. J. L. Pombeiro, *Chem. – Eur. J.*, 2016, **22**, 16356–16398.

17 B. Sridhar, J. B. Nanubolu and K. Ravikumar, *CrystEngComm*, 2012, **14**, 7065–7074.

18 S. R. Perumalla, V. R. Pedireddi and C. C. Sun, *Cryst. Growth Des.*, 2013, **13**, 429–432.

19 S. R. Perumalla, V. R. Pedireddi and C. C. Sun, *Mol. Pharmaceutics*, 2013, **10**, 2462–2466.

20 J. A. Dean, *Lange's Handbook of Chemistry*, McGraw-Hill, New York, NY, 15th edn, 1999.